Chapter 2

Nicotine Binding to Brain Receptors Requires a Strong Cation–π Interaction*

This chapter is adapted in part from:* Xiu, X.[†]; Puskar, N. L.[†]; Shanata, J. A. P.; Lester, H. A.; Dougherty, D. A. Nicotine binding to brain receptors requires a strong cation–π interaction. *Nature*. **2009; *458*: 534-538. *The work described in this chapter concerning varenicline was done in collaboration with Ximena Da Silva Tavares Bongoll, Dr. Angela P. Blum, Darren T. Nakamura, and Dr. Jai A. P. Shanata.*
[†]Denotes equal contribution.

2.1 ABSTRACT

Nicotine addiction begins with high-affinity binding of nicotine to acetylcholine (ACh) receptors in the brain. The end result is over 4,000,000 smoking-related deaths annually worldwide and the largest source of preventable mortality in developed countries. Stress reduction, pleasure, improved cognition and other central nervous system effects are strongly associated with smoking. However, if nicotine activated ACh receptors found in muscle as potently as it does brain ACh receptors, smoking would cause intolerable and perhaps fatal muscle contractions. Despite extensive pharmacological, functional, and structural studies of ACh receptors, the basis for the differential action of nicotine on brain compared with muscle ACh receptors has not been determined. Here we show that at the α4β2 brain receptors thought to underlie nicotine addiction, the high affinity for nicotine binding is the result of a strong cation–π interaction to a specific aromatic amino acid of the receptor, TrpB. In contrast, the low affinity for nicotine at the muscle-type ACh receptor is largely due to the fact that this key interaction is absent, even though the immediate binding site residues, including the

key amino acid TrpB, are identical in the brain and muscle receptors. At the same time a hydrogen bond from nicotine to the backbone carbonyl of TrpB is enhanced in the neuronal receptor relative to the muscle-type. The cation-π interaction and hydrogen bond are also present between TrpB and the smoking cessation compound varenicline (Chantix®) in the α4β2 receptor. Additionally, a point mutation near TrpB that differentiates α4β2 and muscle-type receptors seems to influence the shape of the binding site, allowing nicotine to interact more strongly with TrpB in the neuronal receptor. ACh receptors are established therapeutic targets for Alzheimer's disease, schizophrenia, Parkinson's disease, smoking cessation, pain, attention-deficit hyperactivity disorder, epilepsy, autism, and depression.[1] Along with solving a chemical mystery in nicotine addiction, our results provide guidance for efforts to develop drugs that target specific types of nicotinic receptors.

2.2 INTRODUCTION

Nicotinic acetylcholine receptors (nAChRs) comprise a family of ≥20 homologous subtypes that mediate fast synaptic transmission throughout the central and peripheral nervous systems.[2] The neuronal nAChRs are found in the central nervous system (CNS) and autonomic ganglia. Of these, the subtype most strongly associated with nicotine addiction and the target of recently developed smoking cessation drugs is termed α4β2.[3-7] The high nicotine affinity of α4β2 receptors, when combined with the ability of nicotine to cross the blood–brain barrier and its favourable pharmacokinetics, allows nicotine at the submicromolar concentrations in tobacco smoke to activate acutely these receptors, providing reward, cognitive sensitization, and perhaps other effects. In addition, the high-affinity interaction allows smoked nicotine to act as an intracellular

pharmacological chaperone of α4β2 receptors, leading to the upregulation of receptors thought to underlie effects of chronic exposure.[6-8]

In previous studies of the nAChR of the neuromuscular junction (muscle-type), we showed that an important contributor to ACh binding is a cation-π interaction to a specific tryptophan (called TrpB, residue 149, **Figure 2.1**).[9] These results were subsequently supported by the important series of crystal structures of ACh binding proteins (AChBP).[10, 11] These structures revealed the "aromatic box" structural motif of **Figure 2.1**, and the aligning residues are predominantly aromatic throughout the Cys-loop family of neurotransmitter-gated ion channels. In other Cys-loop receptors, a cation–π interaction between the natural agonist and one of the aromatics is always seen, although its precise location varies.[12] Interestingly, when nicotine activates the muscle-type nAChR, there is no cation–π interaction,[13] consistent with its relatively low affinity for this receptor. This suggested that a cation–π interaction could discriminate between high-affinity neuronal receptors and low-affinity muscle-type receptors. However, subtle effects must be involved, as the nAChRs of the CNS and neuromuscular junction are homologous throughout most regions of sequence and are essentially identical in the immediate vicinity of the agonist binding site (**Figure 2.2**).

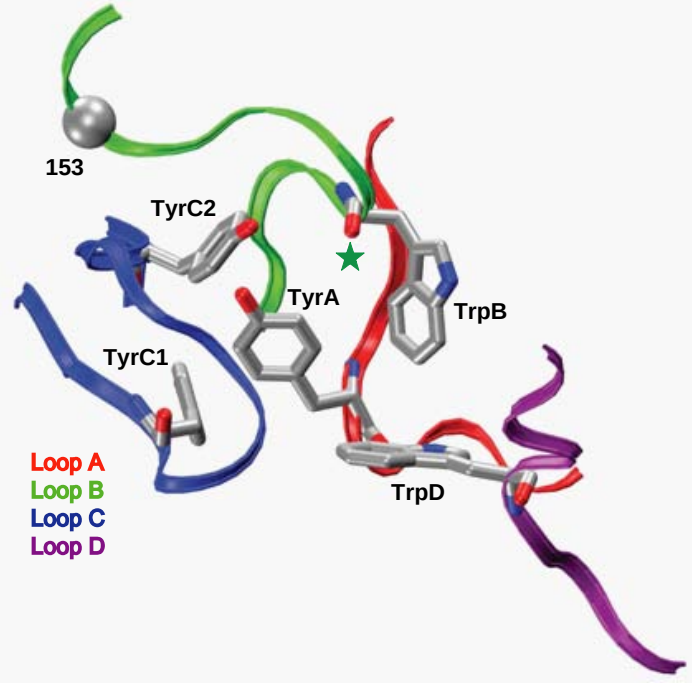

Figure 2.1. The binding site of AChBP, thought to resemble that of nAChRs. Shown are the four principal "loops" that define the binding site.[2] Also highlighted are TrpB (149); its backbone carbonyl (green star); the remaining aromatic residues (TyrA, TyrC1, TyrC, and TrpD); and the α carbon on position 153, which has also been mutated here. The image is of Protein Data Bank file 1I9B.[10]

	Loop A							Loop B							Loop C									
α1 mouse	W	R	P	D	V	V	L	Y	W	T	Y	D	G	S	V	V	Y	S	C	C	P	T	T	P	Y	L	D
α1 human	W	R	P	D	L	V	L	Y	W	T	Y	D	G	S	V	V	Y	S	C	C	P	D	T	P	Y	L	D
α2 human	W	I	P	D	I	V	L	Y	W	T	Y	D	K	A	K	I	Y	D	C	C	A	E	-	I	Y	P	D
α4 human	W	R	P	D	I	V	L	Y	W	T	Y	D	K	A	K	I	Y	E	C	C	A	E	-	I	Y	P	D
α4 rat	W	R	P	D	I	V	L	Y	W	T	Y	D	K	A	K	I	Y	E	C	C	A	E	-	I	Y	P	D
α3 human	W	K	P	D	I	V	L	Y	W	S	Y	D	K	A	K	I	Y	N	C	C	E	E	-	I	Y	P	D
α6 human	W	K	P	D	I	V	L	Y	W	T	Y	D	K	A	E	I	Y	N	C	C	E	E	-	I	Y	T	D
α7 human	W	K	P	D	I	L	L	Y	W	S	Y	G	G	W	S	L	Y	E	C	C	K	E	-	P	Y	P	D
α9 human	W	R	P	D	I	V	L	Y	W	T	Y	N	G	N	Q	V	Y	G	C	C	S	E	-	P	Y	P	D

	Loop D					
γ mouse	W	I	E	M	Q	W
γ human	W	I	E	M	Q	W
δ mouse	W	I	D	H	A	W
δ human	W	I	E	H	G	W
β2 human	W	L	T	Q	E	W
β2 rat	W	L	T	Q	E	W
β3 human	W	L	K	Q	E	W
β4 human	W	L	K	Q	E	W
α7 human	W	L	Q	M	S	W
α9 human	W	I	R	Q	I	W

Figure 2.2. Sequence alignment for loops A, B, C, and D in the vicinity of the aromatic binding box. The five residues of the aromatic box: TyrA, TrpB, TryC1, TyrC2, and TrpD are highlighted in green. They are universally conserved in these subunits. G153 (α1) is the fourth residue after TrpB, highlighted in blue.

Here we describe studies of the neuronal α4β2 receptor. We find a remarkable distinction in binding behaviour: both the endogenous neurotransmitter ACh *and* the addictive nicotine molecule make a strong cation–π interaction to TrpB. In addition, a hydrogen bond from nicotine to the backbone carbonyl of TrpB that is weak in the muscle-type is much stronger in the α4β2 receptor. The smoking cessation drug varenicline (marketed as Chantix® in the U.S.) was designed to target α4β2 receptors,[3, 14, 15] and in fact makes the cation-π interaction and hydrogen bond. Taken together, these two noncovalent interactions fully rationalize the differential affinity of nicotine in the brain *vs.* the neuromuscular junction.

2.3 RESULTS AND DISCUSSION

2.3.1 Challenges in Studying Neuronal nAChRs

A cation–π interaction between a drug and a receptor can be revealed by incorporation of a series of fluorinated amino acid analogues (**Figure 2.3**); a consistent trend in receptor response indicates a binding interaction.[9] Such an experiment is enabled by the nonsense suppression methodology for incorporation of unnatural amino acids into receptors and channels expressed in *Xenopus* oocytes. Although we have found the nonsense suppression methodology to be broadly applicable,[16, 17] implementing the methodology for study of the α4β2 neuronal nAChRs proved to be especially challenging, requiring new strategies. The α4β2 receptors are expressed in *Xenopus* oocytes at inadequately low levels for nonsense suppression experiments. However, recent studies showed that the Leu9'Ala (L9'A) mutation in the M2 transmembrane helix of the α4 subunit greatly improves expression without altering the pharmacological

selectivity of the receptor.[18] (In Cys-loop receptors, the highly homologous M2 sequences are often compared by numbering from the cytoplasmic end, termed position 1'.) Therefore, all studies of α4β2 described here included this mutation. As with other mutations of L9', the L9'A mutation lowers the agonist concentration for half-maximum response (EC_{50}) by influencing receptor gating in ways that are fairly well understood and that do not distort the present analysis of the binding site (some 60 Å from the 9' position).[19, 20] In addition, previous studies of the muscle-type receptor used a comparable mutation at L9', and control experiments established that it did not alter binding trends.[9, 21]

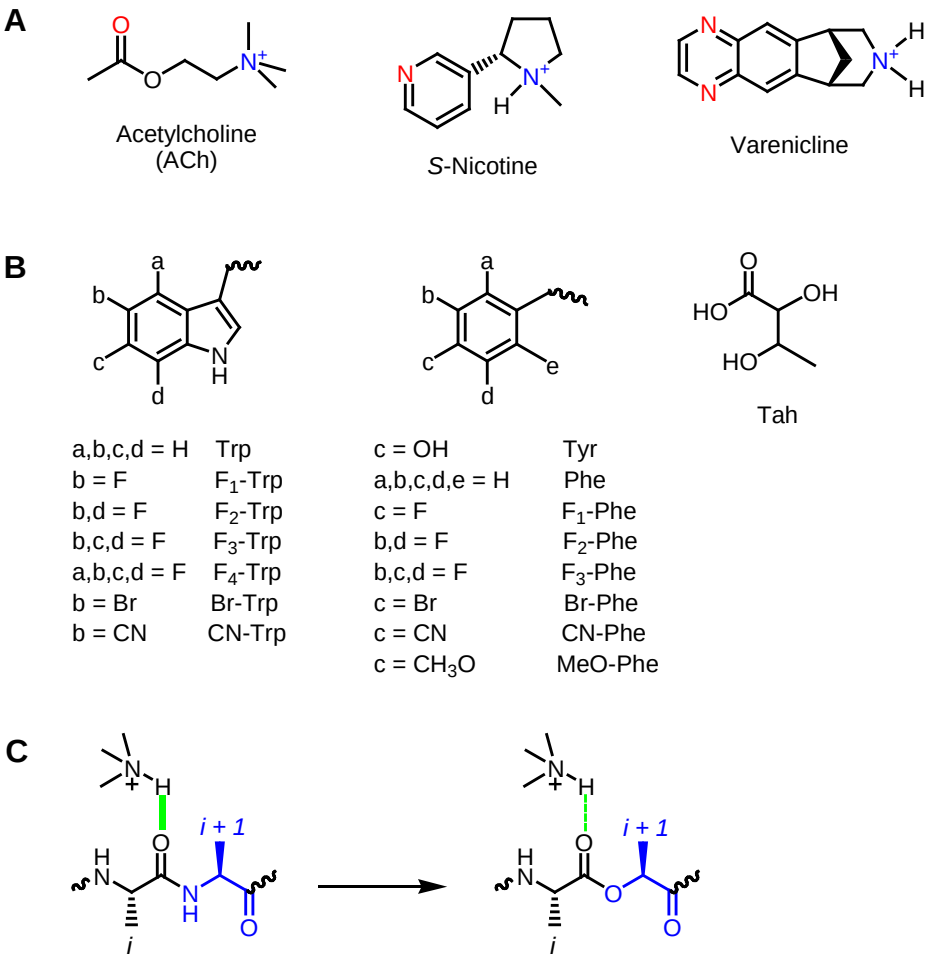

Figure 2.3. Agonists and unnatural amino acids considered here. A. Structures of ACh, nicotine, and varenicline. B. Unnatural amino acids considered here. If not indicated, an a, b, c, or d group is H. Br, bromo group; CN, cyano group; MeO, methoxy group. C. The backbone ester strategy for modulating a hydrogen bond.

The nAChRs are pentameric. The muscle-type receptor has a precise stoichiometry of $(\alpha1)_2\beta1\gamma\delta$, fetal form ($(\alpha1)_2\beta1\varepsilon\delta$); adult form).[2, 22, 23] However, the $\alpha4\beta2$ receptor can have variable stoichiometry. In particular, there are two forms of $\alpha4\beta2$, $(\alpha4)_2(\beta2)_3$ and $(\alpha4)_3(\beta2)_2$, which we refer to hereafter as A2B3 and A3B2, respectively.[8, 24, 25] Agonist binding sites are at the appropriate α–β interfaces. The A2B3 form has higher sensitivity for nicotine and is upregulated during chronic exposure to nicotine; our studies have focused on it. Controlling the ratios of messenger RNAs injected into the oocyte can reliably control subunit stoichiometry in the wild type receptor. Injection of an mRNA subunit ratio $\alpha4$(L9'A):$\beta2$ of 10:1 or higher produces pure populations of A3B2 receptors, while a ratio of 3:1 or lower guarantees a pure population of A2B3 (**Table 2.1**).

Table 2.1. Injection ratio of $\alpha4$(L9'A):$\beta2$ mRNA controls receptor stoichiometry. EC_{50} values (μM) and Hill coefficients (n_H) are shown.

α4L9'A:β2 ratio	**ACh**	**n_H**	**Stoichiometry**
100:1	0.023 ± 0.002	1.5 ± 0.2	A3B2
10:1	0.023 ± 0.001	1.4 ± 0.1	A3B2
6:1	0.15 ± 0.02	0.67 ± 0.04	Mixture
3:1	0.44 ± 0.03	1.2 ± 0.1	A2B3
1:1	0.40 ± 0.01	1.2 ± 0.1	A2B3
1:10	0.43 ± 0.02	1.2 ± 0.1	A2B3

Note that the $\alpha4$(L9'A) mutation lowers EC_{50} in a multiplicative fashion, depending on how many $\alpha4$ subunits are present. As such, our A3B2 receptor (with three L9'A mutations) actually has a lower EC_{50} than our A2B3 receptor (with two L9'A mutations), even though the binding site from the A2B3 stoichiometry is clearly that of the high sensitivity receptor.

In a nonsense suppression experiment, however, the subunit that contains the stop codon where the unnatural amino acid has been incorporated can show low and variable expression levels. Therefore we sought a second, independent indicator of the stoichiometry of the α4β2 receptor. We now report that the A2B3 and A3B2 forms of the α4(L9'A)β2 receptor show markedly different rectification behaviours. As indicated by either voltage ramp or voltage jump experiments, A2B3 is substantially more inward rectifying than A3B2 (**Figure 2.4**). Thus, in all our experiments with unnatural amino acids, the stoichiometries of mutant receptors are monitored by measuring current–voltage relations with voltage jumps. For each mutant receptor studied, we determined the fraction (outward current at +70 mV/inward current at –110 mV), and a value ≤0.1 establishes the desired A2B3 stoichiometry (**Tables 2.2-2.7**). With these methodological developments in hand, incorporation of unnatural amino acids into the α4β2 receptor becomes feasible (**Figure 2.5**).

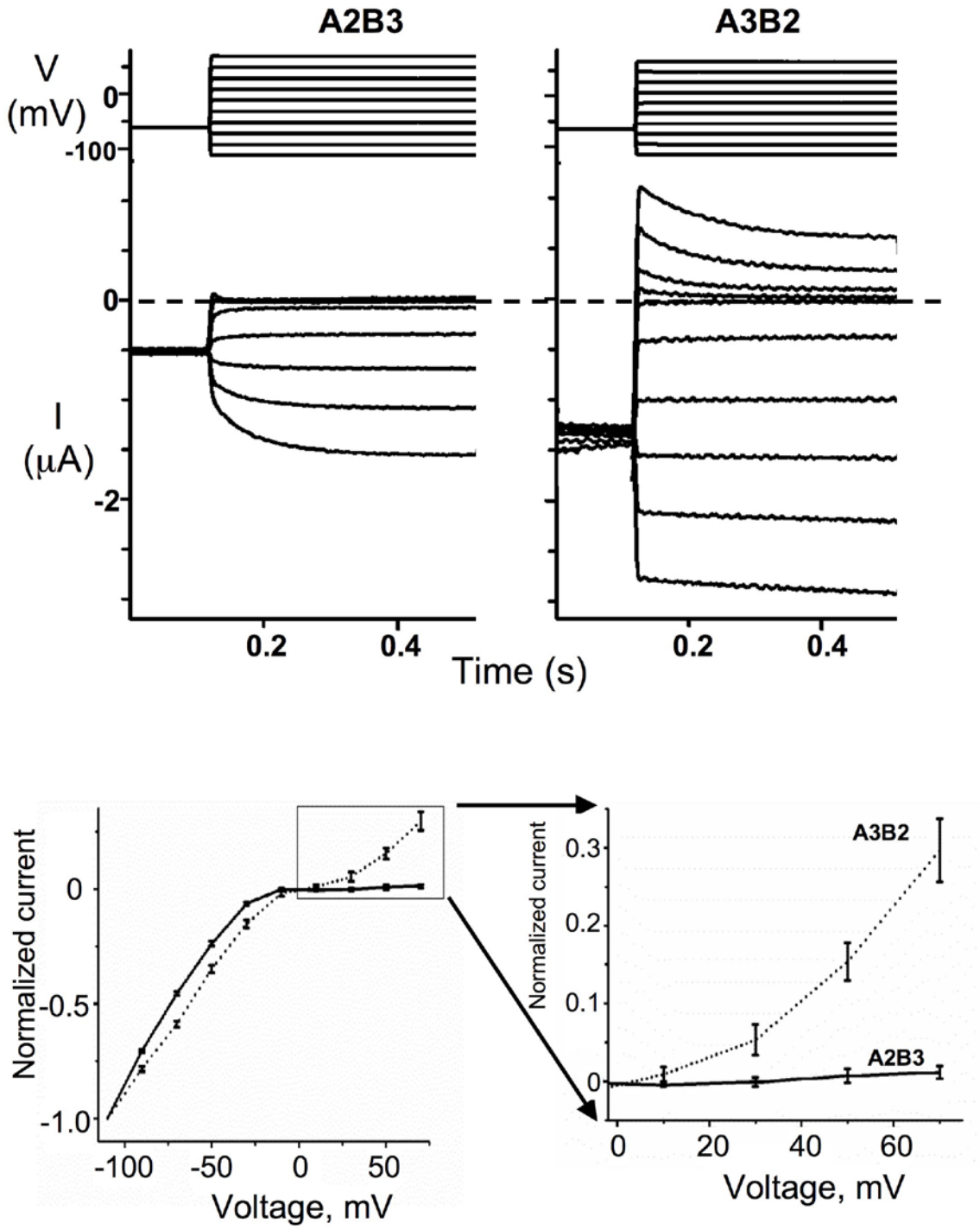

Figure 2.4. Rectification behaviors of A2B3 and A3B2 α4L9'Aβ2 nAChRs. Upper: Representative voltage traces and current responses for voltage jump experiments. Lower: I-V curves for A2B3 (solid line) and A3B2 (dotted line). The inset shows positive voltages, where A2B3 and A3B2 exhibit markedly different behavior.

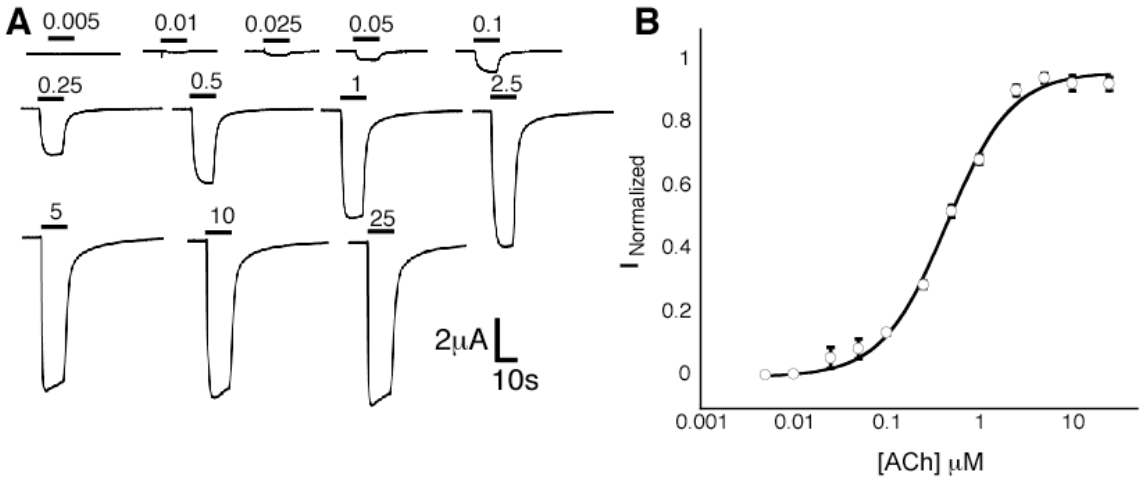

Figure 2.5. Nonsense suppression in the α4β2 receptor. Shown is a wild type recovery experiment, in which Trp is incorporated at the TrpB position. A. Representative traces of voltage-clamp currents. Bars represent application of ACh at concentrations noted (μM). B. Fit of data in A to the Hill equation. Error bars indicate s.e.m.; *n* = 6-8.

2.3.2 TrpB Makes a Cation-π Interaction in the α4β2 Receptor

Given the results with the muscle-type nAChR,[9] a logical starting point to search for a cation-π interaction in the α4β2 receptor is at TrpB (α4Trp149). It is well established that fluorine is deactivating in a cation-π interaction, and that multiple fluorines have an additive effect. If a cation-π interaction is present, successively replacing the wild type aromatic amino acid with monofluoro, difluoro, trifluoro, and tetrafluoro analogues should lead to a systematic increase in EC_{50}. As shown in **Table 2.2** and **Figure 2.6**, a compelling "fluorination" trend is seen for both ACh *and* nicotine at TrpB of the α4β2 receptor. This is in contrast to the results at the muscle-type receptor, in which no such trend is seen for nicotine activation.[9] Further support for an important cation–π interaction for both agonists is provided by the large perturbation induced by a cyano (CN) group—which is strongly deactivating in a cation–π interaction—compared

to a bromo (Br) group, which is roughly isosteric to a cyano group but much less deactivating.

Table 2.2. Functional characterization of TrpB in α4β2 (A2B3). EC_{50} values (μM), Hill coefficients (n_H) and current size at +70 mV (normalized to current size at -110 mV).

Mutation	ACh	n_H	Nicotine	n_H	Norm. I (+70mV)
Wild type					
A2B3	0.42 ± 0.01	1.2 ± 0.1	0.08 ± 0.01	1.2 ± 0.1	0.041 ± 0.005
A3B2	0.023 ± 0.001	1.3 ± 0.1	0.01 ± 0.001	1.7 ± 0.2	0.297 ± 0.041
TrpB A2B3					
Trp	0.44 ± 0.03	1.3 ± 0.1	0.09 ± 0.01	1.5 ± 0.1	0.006 ± 0.014
F_1-Trp	1.9 ± 0.1	1.2 ± 0.1	0.26 ± 0.02	1.3 ± 0.1	-0.065 ± 0.047
F_2-Trp	2.0 ± 0.1	1.3 ± 0.1	0.32 ± 0.04	1.3 ± 0.1	0.032 ± 0.025
F_3-Trp	13 ± 1	1.3 ± 0.1	1.2 ± 0.1	1.4 ± 0.2	-0.073 ± 0.029
F_4-Trp	29 ± 2	1.1 ± 0.1	4.2 ± 0.4	1.3 ± 0.2	-0.027 ± 0.023
CN-Trp	12 ± 1	1.2 ± 0.1	0.90 ± 0.07	1.4 ± 0.1	0.009 ± 0.017
Br-Trp	1.1 ± 0.1	1.3 ± 0.1	0.20 ± 0.02	1.3 ± 0.2	0.020 ± 0.005

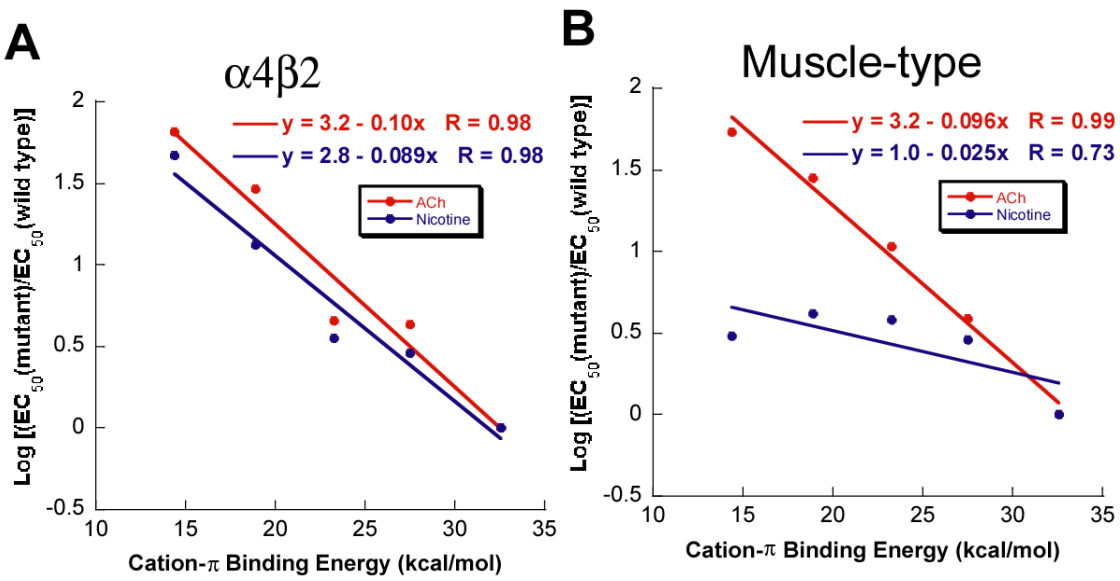

Figure 2.6. Fluorination plots for ACh and nicotine at α4β2 and muscle-type receptors. Note that in both plots, all data sets share the point x = 32.6 kcal/mol (cation-π binding energy for Trp). Moving to the left then corresponds to monofluoro-, difluoro-, trifluoro-, and tetrafluoro-TrpB. ACh (red), nicotine (blue). Cation-π binding energies (x-axes) are from Zhong 1998.[9] A. α4β2 receptor. B. Muscle-type receptor, previously reported in Zhong 1998 and Beene 2002.[9, 13]

The EC_{50} values reported here represent a measure of receptor function; shifts in EC_{50} can result from changes in ligand binding and/or receptor gating properties. By ascribing the results to attenuation of a cation–π interaction, we are effectively concluding that it is agonist binding that is being modulated by fluorination, but that conclusion is not incontrovertible. However, single-channel experiments of α4β2 established that shifts in EC_{50} caused by subtle mutation of TrpB are a consequence of changes in agonist binding, not receptor gating.[26] As such, fluorination of TrpB of the α4β2 (A2B3) receptor primarily has an impact on the sensitivity to nicotine by decreasing nicotine's cation-π interaction with this residue.

2.3.3 TyrA is a Hydrogen Bond Donor in the α4β2 Receptor

The remaining residues (TyrA, TyrC1, and TyrC2) of the aromatic box were also probed with unnatural amino acid mutagenesis. We have found fluorination of tyrosine more challenging than tryptophan because progressive fluorination of tyrosine will lower the pK_a of the side chain hydroxyl group.[27] In fact, the pK_a for tetrafluorotyrosine is ~5.3 (lowered from ~10 for tyrosine) and can induce ionization of the OH in unnatural tyrosine analogues and complicate analysis. To address this issue, we first tested the phenylalanine mutant, and then successively fluorinated phenylalanine derivatives (**Figure 2.3B**), as Phe can be fluorinated without pK_a complications.

TyrA has been extensively studied in many Cys-loop receptors; it was identified as a hydrogen bond donor in the muscle-type receptor and a cation-π binding site in the $GABA_A$ receptor.[27, 28] Here, in the α4β2 receptor, we find that TyrA is sensitive to substituents in the para position for both ACh and nicotine (**Table 2.3**). This indicates that the hydroxyl group is important to channel function, since deletion or substitution

with a cyano, bromo, or fluoro group resulted in a deleterious effect on channel function for both ACh and nicotine. Incorporation of MeO-Phe at TyrA resulted in a 6-fold and 4-fold increase in EC_{50} for ACh and nicotine, respectively, indicating that TyrA is likely a hydrogen bond donor. Furthermore, TyrA is not sensitive to fluorination and therefore neither nicotine nor ACh interact with TyrA via a cation-π interaction.

Table 2.3. Functional characterization of TyrA in α4β2 (A2B3). EC_{50} values (μM), Hill coefficients (n_H) and current size at +70 mV (normalized to current size at -110 mV).

Mutation	ACh	n_H	Nicotine	n_H	Norm. I (+70mV)
Wild type					
A2B3	0.42 ± 0.01	1.2 ± 0.1	0.08 ± 0.01	1.2 ± 0.1	0.041 ± 0.005
A3B2	0.023 ± 0.001	1.3 ± 0.1	0.01 ± 0.001	1.7 ± 0.2	0.297 ± 0.041
TyrA A2B3					
Tyr	0.42 ± 0.03	1.2 ± 0.1	0.08 ± 0.01	1.7 ± 0.3	0.023 ± 0.009
Phe	12 ± 1	1.3 ± 0.1	0.77 ± 0.05	2.1 ± 0.3	0.064 ± 0.011
MeO-Phe	2.3 ± 0.2	1.2 ± 0.1	0.40 ± 0.02	1.7 ± 0.2	0.054 ± 0.032
F_1-Phe	15 ± 1	1.2 ± 0.1	0.32 ± 0.03	1.4 ± 0.2	-0.076 ± 0.046
F_2-Phe	16 ± 2	1.8 ± 0.3	0.39 ± 0.05	1.8 ± 0.4	0.028 ± 0.005
F_3-Phe	14 ± 1	1.2 ± 0.1	0.53 ± 0.04	1.4 ± 0.1	0.044 ± 0.010
Br-Phe	3.3 ± 0.2	1.2 ± 0.1	0.54 ± 0.04	1.5 ± 0.1	-0.003 ± 0.031
CN-Phe	73 ± 4	1.7 ± 0.1	8.8 ± 0.9	1.5 ± 0.2	0.075 ± 0.008

TyrA behaves consistently in both the α4β2 and the muscle-type receptors; however, the importance of this interaction appears to differ for these two receptors. In α4β2, TyrA is much more sensitive to mutations at the para position. With ACh as the agonist, a Tyr to Phe mutation in α4β2 causes a 29-fold increase in EC_{50}, but only a 9-fold increase in the muscle-type receptor. As such, it is likely that the hydrogen bond made by TyrA in α4β2 is more crucial for receptor function than in the muscle-type receptor.

2.3.4 The Functions of TyrC1 and TyrC2 are Conserved in the α4β2 and Muscle-type Receptors

TyrC1 is highly sensitive to any mutation that obliterates hydrogen bond donating ability. This is shown by a rightward shift in EC_{50} of over 100-fold for ACh and over 25-fold for nicotine in response to the Phe, MeO-Phe, and CN-Phe mutations (**Table 2.4**). If TyrC1 function was compromised by a lack of steric bulk, then incorporation of CN-Phe should have returned normal receptor function. Additionally, if this position served as a hydrogen bond acceptor, then incorporation of MeO-Phe should have rescued wild type behavior. However, MeO-Phe incorporation gave a dramatic increase in EC_{50} for both ACh and nicotine, and we therefore conclude that TyrC1 is an important hydrogen bond donor.

Table 2.4. Functional characterization of TyrC1 in α4β2 (A2B3). EC_{50} values (μM), Hill coefficients (n_H) and current size at +70 mV (normalized to current size at -110 mV).

Mutation	ACh	n_H	Nicotine	n_H	Norm. I (+70mV)
Wild type					
A2B3	0.42 ± 0.01	1.2 ± 0.1	0.08 ± 0.01	1.2 ± 0.1	0.041 ± 0.005
A3B2	0.023 ± 0.001	1.3 ± 0.1	0.01 ± 0.001	1.7 ± 0.2	0.297 ± 0.041
TyrC1 A2B3					
Tyr	0.42 ± 0.03	1.5 ± 0.1	0.07 ± 0.01	1.3 ± 0.1	0.042 ± 0.014
Phe	53 ± 4	1.3 ± 0.1	3.3 ± 0.2	1.2 ± 0.1	0.059 ± 0.014
MeO-Phe	48 ± 5	1.4 ± 0.2	2.8 ± 0.4	1.2 ± 0.2	0.064 ± 0.028
CN-Phe	210 ± 10	1.6 ± 0.1	19 ± 2	1.6 ± 0.2	0.057 ± 0.011

In contrast, substitution of TyrC2 displays a strikingly different pattern compared to TyrC1. TyrC2 is extremely permissive to the same mutations tested at TyrC1. All TyrC2 EC_{50} values were essentially unaltered (~1.5-fold shifts in EC_{50}) for both ACh and nicotine (**Table 2.5**). This indicates that TyrC2 primarily serves a structural role in shaping the binding box rather than ligand recognition.

Table 2.5. Functional characterization of TyrC2 in α4β2 (A2B3). EC_{50} values (μM), Hill coefficients (n_H) and current size at +70 mV (normalized to current size at -110 mV).

Mutation	ACh	n_H	Nicotine	n_H	Norm. I (+70mV)
Wild type					
A2B3	0.42 ± 0.01	1.2 ± 0.1	0.08 ± 0.01	1.2 ± 0.1	0.041 ± 0.005
A3B2	0.023 ± 0.001	1.3 ± 0.1	0.01 ± 0.001	1.7 ± 0.2	0.297 ± 0.041
TyrC2 A2B3					
Tyr	0.34 ± 0.01	1.2 ± 0.1	0.08 ± 0.01	1.3 ± 0.1	0.052 ± 0.012
Phe	0.87 ± 0.03	1.3 ± 0.1	0.15 ± 0.01	1.4 ± 0.1	0.039 ± 0.007
MeO-Phe	0.49 ± 0.02	1.3 ± 0.1	0.12 ± 0.01	1.3 ± 0.1	0.033 ± 0.013
CN-Phe	0.64 ± 0.02	1.1 ± 0.1	0.41 ± 0.03	1.1 ± 0.1	0.035 ± 0.009

The results for α4β2 very much parallel our previous findings for the muscle-type receptor. This indicates that it is specifically the interaction with TrpB that discriminates the two receptor subtypes.

2.3.5 A Strong Hydrogen Bond in the α4β2 Receptor

Our results suggest that nicotine is positioned more closely to TrpB in the α4β2 agonist binding site than in the muscle-type. This suggested that another nicotine-binding interaction could also be altered. An important chemical distinction between ACh and nicotine is that only the latter can act as a hydrogen bond donor, through the pyrrolidine N^+-H (**Figure 2.3A**). Examination of the AChBP crystal structures (**Figure 2.1**)[29] suggested that the backbone carbonyl associated with TrpB could act as the hydrogen bond acceptor, and several groups have shown the importance of this interaction.[29-31] Previously, we probed this potential hydrogen bond in the muscle-type receptor by replacing the (*i* + 1) residue with its α-hydroxy analogue (**Figure 2.3C**).[32] This converts the backbone amide to a backbone ester, which is well established to be a substantially poorer hydrogen bond acceptor. In the muscle-type receptor, this change raised the nicotine EC_{50} by a modest factor of 1.6.[32] We now find that for precisely the same change in the α4β2 receptor, the nicotine EC_{50} increases 19-fold, a relatively large effect for such

a subtle mutation.[33-35] Recall that the backbone ester substitution does not destroy the hydrogen bond, it simply attenuates it. Notably, ACh, which cannot make a conventional hydrogen bond to the carbonyl, shows no shift in EC_{50} in response to this mutation (**Table 2.6**). This establishes that the ester mutation does not globally alter the binding/gating characteristics of the receptor.

Table 2.6. Functional characterization of Thr (TrpB + 1) in α4β2 (A2B3). EC_{50} values (μM), Hill coefficients (n_H) and current size at +70 mV (normalized to current size at -110 mV).

Mutation	ACh	n_H	Nicotine	n_H	Norm. I (+70mV)
Wild type					
A2B3	0.42 ± 0.01	1.2 ± 0.1	0.08 ± 0.01	1.2 ± 0.1	0.041 ± 0.005
A3B2	0.023 ± 0.001	1.3 ± 0.1	0.01 ± 0.001	1.7 ± 0.2	0.297 ± 0.041
Thr (TrpB+1) A2B3					
Thr	0.41 ± 0.02	1.4 ± 0.1	0.09 ± 0.01	1.6 ± 0.1	0.044 ± 0.007
Tah	0.37 ± 0.02	1.3 ± 0.1	1.71 ± 0.14	1.2 ± 0.1	0.018 ± 0.013

2.3.6 Studies with the Smoking Cessation Drug Varenicline at the α4β2 Receptor

We also evaluated the agonist binding mode of varenicline, a smoking cessation drug. Varenicline (marketed by Pfizer as Chantix® in the U.S.) was designed to target α4β2 receptors, and was approved for use in smoking cessation in 2006.[3] Using the fluorination approach and the CN/Br effect, we show that varenicline, like nicotine, binds to TrpB of the α4β2 receptor via a cation-π interaction (**Table 2.7, Figure 2.7**).

Table 2.7. Functional characterization of varenicline at TrpB in α4β2 (A2B3). EC_{50} values (μM), Hill coefficients (n_H) and current size at +70 mV (normalized to current size at -110 mV).

Mutation	Varenicline	n_H	Norm. I (+70mV)
Wild type			
A2B3	2.9 ± 0.1	1.4 ± 0.1	0.037 ± 0.007
A3B2	0.75 ± 0.06	1.4 ± 0.1	0.166 ± 0.014
TrpB A2B3			
Trp	2.4 ± 0.2	1.2 ± 0.1	0.043 ± 0.005
F_1-Trp	5.7 ± 0.2	1.2 ± 0.1	0.040 ± 0.007
F_2-Trp	9.0 ± 0.4	1.2 ± 0.1	0.050 ± 0.011
F_3-Trp	27 ± 1	1.3 ± 0.1	0.044 ± 0.009
F_4-Trp	56 ± 5	1.1 ± 0.1	0.033 ± 0.008
Br-Trp	7.1 ± 0.5	1.1 ± 0.1	0.039 ± 0.007
CN-Trp	31 ± 2	1.1 ± 0.1	0.040 ± 0.009

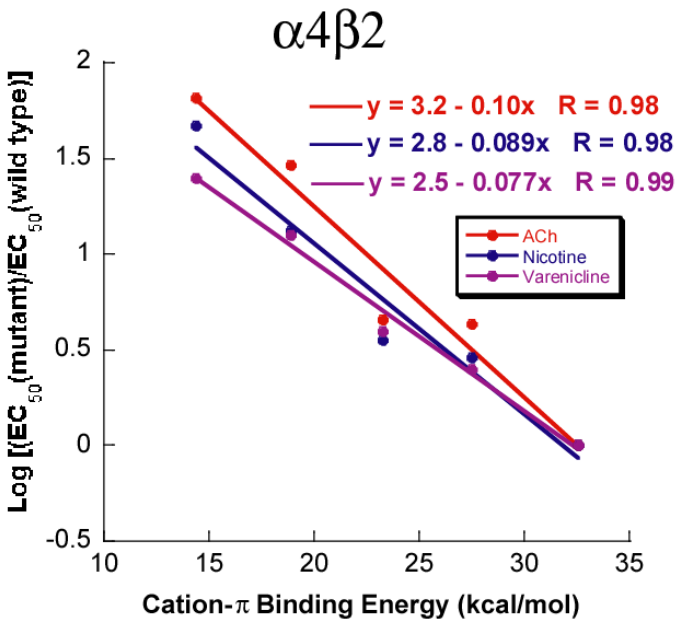

Figure 2.7. Fluorination plot for varenicline at α4β2 (A2B3). All data sets share the point x = 32.6 kcal/mol (cation-π binding energy for Trp). Moving to the left then corresponds to monofluoro-, difluoro-, trifluoro-, and tetrafluoro-TrpB. ACh (red), nicotine (blue), varenicline (purple). Cation-π binding energies (x-axes) are from Zhong 1998.[9]

We have previously argued that the magnitude of the perturbation to EC_{50} induced by fluorination can be taken as an indicator of the relative strength of a cation-π

interaction. In **Table 2.8** we characterize the strength of a cation-π interaction by the ratio of EC_{50} values for the F_4-Trp mutant *vs.* the wild type. The F_4-Trp residue represents a side chain in which the electrostatic component of the cation-π interaction has been completely removed, but other features of the residue are essentially intact (**Figure 2.8**). All drug-receptor pairings reported here show a significant "cation-π ratio," thus establishing a common anchor point for the binding of the drugs considered here to the α4β2 receptor.

Table 2.8. Evaluation of binding interactions in the α4β2 (A2B3) receptor. a. Values are corrected for the effects of α4L9'A mutation according to the procedure of Moroni *et al.*[24] As such, these are EC_{50} for true wild type receptors. b. Ratio of EC_{50} values for F_4-Trp/Trp at position TrpB in α4. c. Ratio of EC_{50} values for Tah/Thr at position Thr (TrpB + 1) in α4.

	Measured EC_{50} (μM)	**Wild type EC_{50} (μM)[a]**	**Cation-π interaction[b]**	**N^+–H•••O=C (Backbone H-bond)[c]**
ACh	0.42	4.0	69	1.1
Nicotine	0.08	0.76	53	19
Varenicline	0.00285	0.027	20	14

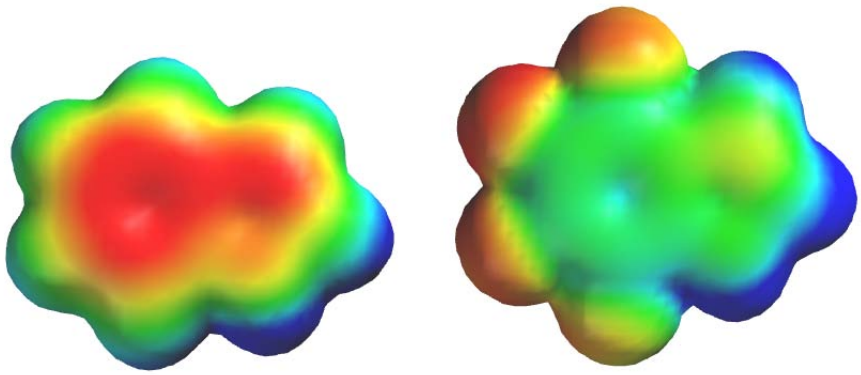

Figure 2.8. Electrostatic potential surfaces of indole (left) and F_4-indole, corresponding to the aromatic portions of the side chains of Trp and F_4-Trp, respectively. Results are from HF-6-31G** calculations. Electrostatic potential ranges from -25 kcal/mol (red) to +25 kcal/mol (blue), so that green represents ~0 electrostatic potential.

Using the backbone amide-to-ester strategy for perturbing a hydrogen bond, we examined whether the N^+H moiety of varenicline functions as a hydrogen bond donor to α4β2. Replacing the (TrpB + 1) residue, which is threonine with threonine-α-hydroxy (Tah) significantly impacts EC_{50}, suggesting the hydrogen bond donor interaction to the backbone carbonyl of TrpB is significant. To facilitate comparison, we have expressed variations as a ratio of EC_{50} values, comparing the receptor with Tah at residue the (TrpB + 1) residue to the wild type Thr (**Table 2.9**). Varenicline, like nicotine, shows an EC_{50} ratio significantly greater than 1, with only modest variations in magnitude (**Table 2.8**).

Table 2.9. Functional characterization of varenicline at Thr (TrpB + 1) in α4β2 (A2B3). EC_{50} values (μM), Hill coefficients (n_H) and current size at +70 mV (normalized to current size at -110 mV).

Mutation	Varenicline	n_H	Norm. I (+70mV)
Wild type			
A2B3	2.9 ± 0.1	1.4 ± 0.1	0.037 ± 0.007
A3B2	0.75 ± 0.06	1.4 ± 0.1	0.166 ± 0.014
Thr (TrpB + 1) A2B3			
Thr	2.2 ± 0.1	1.3 ± 0.1	0.020 ± 0.002
Tah	30 ± 2	1.2 ± 0.1	0.029 ± 0.006

2.3.7 A Residue Outside of the Aromatic Box Differentiates the α4β2 and Muscle-type Receptors

The differential affinity of nicotine for α4β2 versus muscle-type receptors results from stronger interactions in the former with TrpB—both cation–π and hydrogen bonding. Because the two receptors are identical with regard to the five residues that make up the aromatic box, a factor "outside the box" must be influencing its precise geometry, such that nicotine can approach TrpB more closely in α4β2 than in muscle-type nAChR. Pioneering work has identified residues responsible for the fact that α4β2 receptors show consistently higher affinity than the homopentameric α7 neuronal

receptors.[36] At a particular residue in loop B—position 153, just four residues from TrpB—mutations strongly influence affinity. In high-affinity α4β2 receptors this residue is a Lys, and this residue is proposed to help shape the aromatic box by forming a backbone hydrogen bond between loops B and C (**Figure 2.1**). In the lower affinity α7 neuronal receptor, residue 153 is a Gly, and molecular dynamics simulations of α7 suggest that a Gly at 153 discourages the formation of the hydrogen bond between loops B and C.[36] Interestingly, the aligning residue in the muscle-type receptor is also Gly, and a naturally occurring G153S mutation is gain-of-function and associated with a congenital myasthenic syndrome.[37] We now report that the muscle-type α1 G153K mutant shows much higher affinity for nicotine, and that, when this mutation is present, the cation–π interaction to TrpB is strong. The data are summarized in **Table 2.10** and **Figure 2.9**. As expected, the ACh cation–π interaction is maintained in the muscle-type receptor with the G153K mutation. These data indicate that the loop B–loop C hydrogen bond that is naturally present in α4β2 shapes the aromatic box so that nicotine can make a closer contact to TrpB, and that this structural feature is absent or weaker in the muscle-type receptor.

Table 2.10. Functional characterization of the muscle-type receptor containing the G153K point mutation in the α1 subunit. EC_{50} values (μM), Hill coefficients (n_H). All studies of the muscle-type receptor contain a L9'S mutation in the β subunit.

Mutation	ACh	n_H	Nicotine	n_H
Conventional Mutagenesis				
α1G153K	0.021 ± 0.001	1.3 ± 0.1	0.76 ± 0.05	1.7 ± 0.2
TrpB Muscle-type (α1G153K)				
Trp	0.019 ± 0.001	1.5 ± 0.1	0.59 ± 0.04	1.8 ± 0.2
F_1-Trp	0.094 ± 0.004	1.6 ± 0.1	2.8 ± 0.1	1.3 ± 0.1
F_2-Trp	0.079 ± 0.004	1.3 ± 0.1	2.3 ± 0.1	1.3 ± 0.1
F_3-Trp	1.05 ± 0.03	1.3 ± 0.1	11 ± 1	1.5 ± 0.1
F_4-Trp	7.5 ± 0.5	1.2 ± 0.1	32 ± 4	1.5 ± 0.2
CN-Trp	2.4 ± 0.1	1.5 ± 0.1	36 ± 3	1.7 ± 0.2
Br-Trp	0.047 ± 0.001	1.4 ± 0.1	4.5 ± 0.4	1.2 ± 0.1

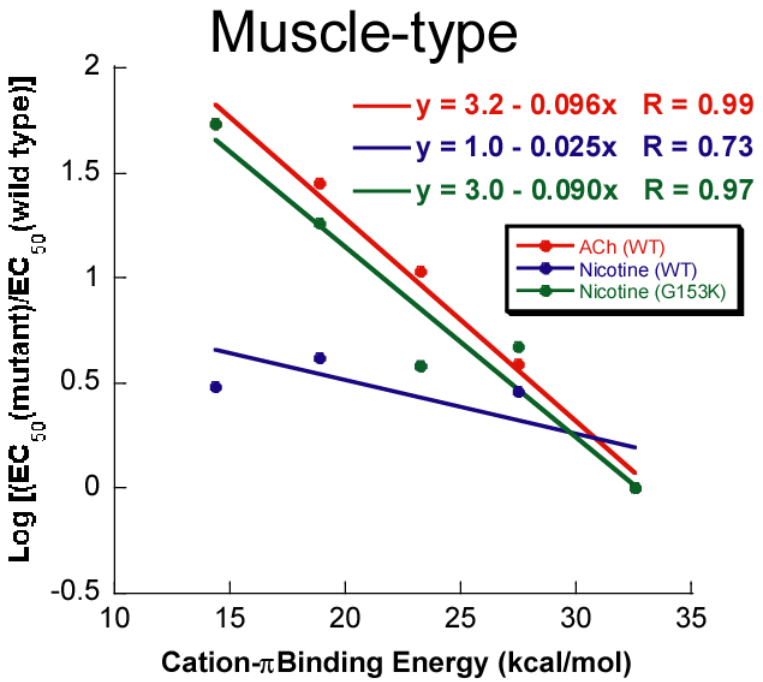

Figure 2.9. Fluorination plot testing nicotine at the muscle-type receptor containing the G153K point mutation in the α1 subunit. All data sets share the point *x* = 32.6 kcal/mol (cation-π binding energy for Trp). Moving to the left then corresponds to monofluoro-, difluoro-, trifluoro-, and tetrafluoro-TrpB. ACh at the WT receptor (red), nicotine at the WT receptor (blue), previously reported in Zhong 1998 and Beene 2002.[9, 13] WT indicates glycine at position 153. Nicotine at the α1G153K receptor (green). Cation-π binding energies (*x*-axes) are from Zhong 1998.[9]

2.3.8 Summary

Taken together, the present results indicate that the higher affinity of nicotine in the brain relative to the neuromuscular junction is a consequence of enhanced interactions with TrpB. A cation–π interaction that is absent in the muscle-type receptor is quite strong in α4β2. In addition, a hydrogen bond to a backbone carbonyl that is weak in the muscle-type is enhanced in α4β2. Varenicline, the smoking cessation drug designed to target α4β2 receptors and block nicotine binding, also employ the same cation-π and hydrogen bonding interactions. Both effects are quite substantial, and in combination they are more than adequate to account fully for the differential sensitivity to nicotine of the two receptors. The side chain of residue 153 in loop B distinguishes the two receptor types and apparently influences the shape of the binding site aromatic box, allowing a stronger interaction between nicotine and TrpB in high-affinity receptors.

2.4 METHODS

mRNA Synthesis and Mutagenesis

All nAChR subunit genes were in the pAMV vector (rat α4 and β2; mouse α1, β1, γ and δ). nAChR subunit mRNA was obtained from NotI linearizations of the expression vector pAMV, followed by *in vitro* transcription using the mMessage mMachine T7 kit (Ambion, Austin, TX). The mutations for each subunit were introduced according to the QuikChange mutagenesis protocol (Stratagene, La Jolla, CA).

Ion Channel Expression

To express the ion channels with a wild type ligand binding box, α4L9'A mRNA was coinjected with β2 mRNA at various ratios, see **Table 2.1** (total mRNA 10-

25 ng/cell). For muscle-type nAChR experiments, α1:β1:γ:δ mRNA was injected at a ratio of 2:1:1:1 by mass for wild type protein. Note that for all experiments reported, we use a previously reported L9'S mutation in the β1 subunit to increase receptor sensitivity.[9] For nonsense suppression experiments of the muscle-type receptor, an mRNA ratio of 10:1:1:1 was employed. For wild type and nonsense suppression experiments, the total mRNA injected was 30-65 ng/oocyte. Stage V-VI oocytes *Xenopus laevis* were injected and incubated in ND96 solution (96 mM NaCl, 2 mM KCl, 1 mM $MgCl_2$, 1.8 mM $CaCl_2$, and 5 mM HEPES, pH 7.5) with 0.005% (w/v) gentamycin and 2% (v/v) horse serum at 18 °C for 24-48 hours.

Unnatural Amino Acid / α-hydroxy Acid Incorporation

Nitroveratryloxycarbonyl (NVOC) protected cyanomethyl ester form of unnatural amino acids and α-hydroxythreonine cyanomethyl ester were synthesized, coupled to the dinucleotide dCA, and enzymatically ligated to 74-mer THG73 $tRNA_{CUA}$.[17, 38] The unnatural amino acid-conjugated tRNA was deprotected by photolysis immediately prior to coinjection with mRNA containing the UAG mutation at the site of interest. Approximately 10-25 ng mRNA and 25 ng tRNA-amino acid or tRNA-hydroxy acid were injected into stage V–VI oocytes in a total volume of 70 nL.

The fidelity of unnatural amino acid incorporation was confirmed at each site with a "wild type recovery" experiment and a "read-through/reaminoacylation" test. In the "wild type recovery" experiment, UAG mutant mRNA was coinjected with tRNA charged with the amino acid that is present at this residue in the wild type protein. Generation of receptors that were indistinguishable from the wild type protein indicated that the residue carried by the suppressor tRNA was successfully and exclusively

integrated into the protein. In the “read-through/reaminoacylation” test, the UAG mutant mRNA was introduced with (1) no tRNA, (2) tRNA THG73 that was not charged with any amino acid or (3) tRNA THG73 enzymatically ligated with dinucleotide dCA. Lack of currents in these experiments validated the reliability of the nonsense suppression experiments.

Whole-Cell Electrophysiological Characterization of Ion Channels

Agonist-induced currents were recorded in two-electrode voltage clamp mode using the OpusXpress 6000A (Molecular Devices Axon Instruments) at a holding potential of -60 mV. Agonists were prepared in Ca^{2+}-free ND96 solution and applied for 12 seconds followed by a 2 minute wash with Ca^{2+}-free ND96 solution between each concentration. Acetylcholine chloride and (-)-nicotine tartrate were purchased from Sigma/Aldrich/RBI (St. Louis, MO). Varenicline tartrate was obtained from Targacept. Dose-response data were obtained for at least 6 concentrations of agonists and for a minimum of 5 oocytes. Mutants with I_{max} of at least 100 nA of current were defined as functional. EC_{50} and Hill coefficient were calculated by fitting the dose-response relation to the Hill equation. All data are reported as mean ± SE.

Voltage jump experiments were performed in the absence of ACh and at EC_{50} concentration of ACh. The membrane potential was held at -60 mV, and stepped to 10 test potentials at 20 mV increments between +70 mV and -110 mV for 400 ms each. 600 ms at the -60 mV holding potential was allowed between each test potential. Background traces (no ACh) were subtracted from data traces, which were used to measure the steady-state amplitudes of the ACh-induced currents approaching the end of the test pulses. Normalized I-V curves were generated using current amplitudes

normalized to that at -110 mV. For each α4L9'Aβ2 mutant, normalized $I_{+70\ mV} \pm$ SE from at least 5 cells was reported.

2.5 ACKNOWLEDGEMENTS

We thank B. N. Cohen for advice on single-channel recording and analysis. This work was supported by the NIH (NS 34407; NS 11756) and the California Tobacco-Related Disease Research Program of the University of California, grant number 16RT-0160. J.A.P.S. was partially supported by an NRSA training grant. Varenicline tartrate was a generous gift from Targacept.

2.6 REFERENCES

1. Romanelli, M. N.; Gratteri, P.; Guandalini, L.; Martini, E.; Bonaccini, C.; Gualtieri, F., Central Nicotinic Receptors: Structure, Function, Ligands, and Therapeutic Potential. *ChemMedChem* **2007,** 2, (6), 746-767.
2. Corringer, P. J.; Le Novere, N.; Changeux, J. P., Nicotinic receptors at the amino acid level. *Annu Rev Pharmacol Toxicol* **2000,** 40, 431-58.
3. Coe, J. W.; Brooks, P. R.; Vetelino, M. G.; Wirtz, M. C.; Arnold, E. P.; Huang, J.; Sands, S. B.; Davis, T. I.; Lebel, L. A.; Fox, C. B.; Shrikhande, A.; Heym, J. H.; Schaeffer, E.; Rollema, H.; Lu, Y.; Mansbach, R. S.; Chambers, L. K.; Rovetti, C. C.; Schulz, D. W.; Tingley, F. D., 3rd; O'Neill, B. T., Varenicline: an alpha4beta2 nicotinic receptor partial agonist for smoking cessation. *J Med Chem* **2005,** 48, (10), 3474-7.
4. Gotti, C.; Zoli, M.; Clementi, F., Brain nicotinic acetylcholine receptors: native subtypes and their relevance. *Trends Pharmacol Sci* **2006,** 27, (9), 482-91.
5. Mansvelder, H. D.; Keath, J. R.; McGehee, D. S., Synaptic mechanisms underlie nicotine-induced excitability of brain reward areas. *Neuron* **2002,** 33, (6), 905-19.
6. Tapper, A. R.; McKinney, S. L.; Nashmi, R.; Schwarz, J.; Deshpande, P.; Labarca, C.; Whiteaker, P.; Marks, M. J.; Collins, A. C.; Lester, H. A., Nicotine activation of alpha4* receptors: sufficient for reward, tolerance, and sensitization. *Science* **2004,** 306, (5698), 1029-32.
7. Nashmi, R.; Xiao, C.; Deshpande, P.; McKinney, S.; Grady, S. R.; Whiteaker, P.; Huang, Q.; McClure-Begley, T.; Lindstrom, J. M.; Labarca, C.; Collins, A. C.; Marks, M. J.; Lester, H. A., Chronic nicotine cell specifically upregulates functional alpha 4* nicotinic receptors: basis for both tolerance in midbrain and enhanced long-term potentiation in perforant path. *J Neurosci* **2007,** 27, (31), 8202-18.
8. Kuryatov, A.; Luo, J.; Cooper, J.; Lindstrom, J., Nicotine acts as a pharmacological chaperone to up-regulate human alpha4beta2 acetylcholine receptors. *Mol Pharmacol* **2005,** 68, (6), 1839-51.
9. Zhong, W.; Gallivan, J. P.; Zhang, Y.; Li, L.; Lester, H. A.; Dougherty, D. A., From ab initio quantum mechanics to molecular neurobiology: a cation-pi binding site in the nicotinic receptor. *Proc Natl Acad Sci U S A* **1998,** 95, (21), 12088-93.
10. Brejc, K.; van Dijk, W. J.; Klaassen, R. V.; Schuurmans, M.; van Der Oost, J.; Smit, A. B.; Sixma, T. K., Crystal structure of an ACh-binding protein reveals the ligand-binding domain of nicotinic receptors. *Nature* **2001,** 411, (6835), 269-76.
11. Sixma, T. K.; Smit, A. B., Acetylcholine binding protein (AChBP): a secreted glial protein that provides a high-resolution model for the extracellular domain of pentameric ligand-gated ion channels. *Annu Rev Biophys Biomol Struct* **2003,** 32, 311-34.
12. Dougherty, D. A., Cys-loop neuroreceptors: structure to the rescue? *Chem Rev* **2008,** 108, (5), 1642-53.
13. Beene, D. L.; Brandt, G. S.; Zhong, W.; Zacharias, N. M.; Lester, H. A.; Dougherty, D. A., Cation-pi interactions in ligand recognition by serotonergic (5-HT3A) and nicotinic acetylcholine receptors: the anomalous binding properties of nicotine. *Biochemistry* **2002,** 41, (32), 10262-9.

14. Gonzales, D.; Rennard, S. I.; Nides, M.; Oncken, C.; Azoulay, S.; Billing, C. B.; Watsky, E. J.; Gong, J.; Williams, K. E.; Reeves, K. R., Varenicline, an alpha4beta2 nicotinic acetylcholine receptor partial agonist, vs sustained-release bupropion and placebo for smoking cessation: a randomized controlled trial. *JAMA* **2006,** 296, (1), 47-55.
15. Mihalak, K. B.; Carroll, F. I.; Luetje, C. W., Varenicline is a partial agonist at alpha4beta2 and a full agonist at alpha7 neuronal nicotinic receptors. *Mol Pharmacol* **2006,** 70, (3), 801-5.
16. Dougherty, D. A., Physical organic chemistry on the brain. *J Org Chem* **2008,** 73, (10), 3667-73.
17. Nowak, M. W.; Gallivan, J. P.; Silverman, S. K.; Labarca, C. G.; Dougherty, D. A.; Lester, H. A., In vivo incorporation of unnatural amino acids into ion channels in Xenopus oocyte expression system. *Methods Enzymol* **1998,** 293, 504-29.
18. Fonck, C.; Cohen, B. N.; Nashmi, R.; Whiteaker, P.; Wagenaar, D. A.; Rodrigues-Pinguet, N.; Deshpande, P.; McKinney, S.; Kwoh, S.; Munoz, J.; Labarca, C.; Collins, A. C.; Marks, M. J.; Lester, H. A., Novel seizure phenotype and sleep disruptions in knock-in mice with hypersensitive alpha 4* nicotinic receptors. *J Neurosci* **2005,** 25, (49), 11396-411.
19. Filatov, G. N.; White, M. M., The role of conserved leucines in the M2 domain of the acetylcholine receptor in channel gating. *Mol Pharmacol* **1995,** 48, (3), 379-84.
20. Labarca, C.; Nowak, M. W.; Zhang, H.; Tang, L.; Deshpande, P.; Lester, H. A., Channel gating governed symmetrically by conserved leucine residues in the M2 domain of nicotinic receptors. *Nature* **1995,** 376, (6540), 514-6.
21. Kearney, P. C.; Nowak, M. W.; Zhong, W.; Silverman, S. K.; Lester, H. A.; Dougherty, D. A., Dose-response relations for unnatural amino acids at the agonist binding site of the nicotinic acetylcholine receptor: tests with novel side chains and with several agonists. *Mol Pharmacol* **1996,** 50, (5), 1401-12.
22. Grutter, T.; Changeux, J. P., Nicotinic receptors in wonderland. *Trends Biochem Sci* **2001,** 26, (8), 459-63.
23. Karlin, A., Emerging structure of the nicotinic acetylcholine receptors. *Nat Rev Neurosci* **2002,** 3, (2), 102-14.
24. Moroni, M.; Zwart, R.; Sher, E.; Cassels, B. K.; Bermudez, I., alpha4beta2 nicotinic receptors with high and low acetylcholine sensitivity: pharmacology, stoichiometry, and sensitivity to long-term exposure to nicotine. *Mol Pharmacol* **2006,** 70, (2), 755-68.
25. Nelson, M. E.; Kuryatov, A.; Choi, C. H.; Zhou, Y.; Lindstrom, J., Alternate stoichiometries of alpha4beta2 nicotinic acetylcholine receptors. *Mol Pharmacol* **2003,** 63, (2), 332-41.
26. Xiu, X.; Puskar, N. L.; Shanata, J. A.; Lester, H. A.; Dougherty, D. A., Nicotine binding to brain receptors requires a strong cation-pi interaction. *Nature* **2009,** 458, (7237), 534-7.
27. Nowak, M. W.; Kearney, P. C.; Sampson, J. R.; Saks, M. E.; Labarca, C. G.; Silverman, S. K.; Zhong, W.; Thorson, J.; Abelson, J. N.; Davidson, N.; et al., Nicotinic receptor binding site probed with unnatural amino acid incorporation in intact cells. *Science* **1995,** 268, (5209), 439-42.

28. Padgett, C. L.; Hanek, A. P.; Lester, H. A.; Dougherty, D. A.; Lummis, S. C., Unnatural amino acid mutagenesis of the GABA(A) receptor binding site residues reveals a novel cation-pi interaction between GABA and beta 2Tyr97. *J Neurosci* **2007,** 27, (4), 886-92.
29. Celie, P. H.; van Rossum-Fikkert, S. E.; van Dijk, W. J.; Brejc, K.; Smit, A. B.; Sixma, T. K., Nicotine and carbamylcholine binding to nicotinic acetylcholine receptors as studied in AChBP crystal structures. *Neuron* **2004,** 41, (6), 907-14.
30. Hansen, S. B.; Sulzenbacher, G.; Huxford, T.; Marchot, P.; Taylor, P.; Bourne, Y., Structures of Aplysia AChBP complexes with nicotinic agonists and antagonists reveal distinctive binding interfaces and conformations. *EMBO J* **2005,** 24, (20), 3635-46.
31. Talley, T. T.; Yalda, S.; Ho, K. Y.; Tor, Y.; Soti, F. S.; Kem, W. R.; Taylor, P., Spectroscopic analysis of benzylidene anabaseine complexes with acetylcholine binding proteins as models for ligand-nicotinic receptor interactions. *Biochemistry* **2006,** 45, (29), 8894-902.
32. Cashin, A. L.; Petersson, E. J.; Lester, H. A.; Dougherty, D. A., Using physical chemistry to differentiate nicotinic from cholinergic agonists at the nicotinic acetylcholine receptor. *J Am Chem Soc* **2005,** 127, (1), 350-6.
33. Deechongkit, S.; Nguyen, H.; Powers, E. T.; Dawson, P. E.; Gruebele, M.; Kelly, J. W., Context-dependent contributions of backbone hydrogen bonding to beta-sheet folding energetics. *Nature* **2004,** 430, (6995), 101-5.
34. England, P. M.; Zhang, Y.; Dougherty, D. A.; Lester, H. A., Backbone mutations in transmembrane domains of a ligand-gated ion channel: implications for the mechanism of gating. *Cell* **1999,** 96, (1), 89-98.
35. Koh, J. T.; Cornish, V. W.; Schultz, P. G., An experimental approach to evaluating the role of backbone interactions in proteins using unnatural amino acid mutagenesis. *Biochemistry* **1997,** 36, (38), 11314-22.
36. Grutter, T.; Prado de Carvalho, L.; Le Novere, N.; Corringer, P. J.; Edelstein, S.; Changeux, J. P., An H-bond between two residues from different loops of the acetylcholine binding site contributes to the activation mechanism of nicotinic receptors. *EMBO J* **2003,** 22, (9), 1990-2003.
37. Sine, S. M.; Ohno, K.; Bouzat, C.; Auerbach, A.; Milone, M.; Pruitt, J. N.; Engel, A. G., Mutation of the acetylcholine receptor alpha subunit causes a slow-channel myasthenic syndrome by enhancing agonist binding affinity. *Neuron* **1995,** 15, (1), 229-39.
38. Saks, M. E.; Sampson, J. R.; Nowak, M. W.; Kearney, P. C.; Du, F.; Abelson, J. N.; Lester, H. A.; Dougherty, D. A., An engineered Tetrahymena tRNAGln for in vivo incorporation of unnatural amino acids into proteins by nonsense suppression. *J Biol Chem* **1996,** 271, (38), 23169-75.